

## Recrystallization during Alpha+Beta Processing of IMI834

Phuong Vo<sup>1</sup>, Mohammad Jahazi<sup>2</sup>, Stephen Yue<sup>1</sup>

<sup>1</sup>Department of Metals and Materials Engineering, McGill University, 3610 University Street, Montreal, QC, Canada H3A 2B2

<sup>2</sup>Aerospace Manufacturing Technology Center, Institute for Aerospace Research, National Research Council Canada, 5145 Decelles, Montreal, QC, Canada H3T 2B2

The flow behavior and microstructure development of a near- $\alpha$  titanium alloy during processing in the two-phase  $\alpha+\beta$  temperature regime has been investigated. Typical cogging conditions were simulated through compression testing of IMI834 with an initial bimodal  $\alpha+\beta$  microstructure at temperatures of 1248K-1298K, strain rates of  $0.01\text{s}^{-1}$ - $1\text{s}^{-1}$  and post-deformation heat treatments up to 60min. Dynamic recrystallization occurs during forging in the upper range of the two-phase  $\alpha+\beta$  temperature regime ( $\geq 1273\text{K}$ ) and is greater in comparison to the  $\beta$  forging temperature regime. At high  $\alpha+\beta$  temperatures, recovery is less effective and the presence of equiaxed  $\alpha$  grains limits the pre-deformation prior- $\beta$  grain size. Deformation at lower two-phase temperatures (1248K) results in shearing/globularization of lamellar  $\alpha$ , which is retained from the as-received microstructure.

**Keywords:** recrystallization, hot working, near-alpha IMI834

### 1. Introduction

Thermomechanical processing (TMP) of near- $\alpha$  titanium alloys such as IMI834 involves a series of deformation stages above and below the  $\beta \rightarrow \alpha+\beta$  transformation temperature ( $\beta$  transus) and is employed as a means of microstructural control. In particular, TMP is performed to achieve grain refinement and modification of phase morphology through  $\beta$  recrystallization and  $\alpha$  globularization mechanisms. However there exists a wide variation in scale, morphology and distribution of  $\alpha$  and  $\beta$  phases during deformation, translating into a multitude of variables to track. As this renders precise control difficult to achieve in practice, the ability to improve forging quality hinders on the characterization of microstructure development during TMP and has been an area of significant research<sup>1-3</sup>.

The quantitative characterization and modeling of flow behavior and microstructure development during processing at one-phase  $\beta$  temperatures have been previously investigated with regard to recrystallization<sup>4</sup>. During  $\beta$  working, dynamic recrystallization was not significant (<10%) and metadynamic/static recrystallization is necessary to achieve refined microstructures. Deformation in the two-phase  $\alpha+\beta$  temperature region is currently being modeled quantitatively with regard to the size and aspect ratio of prior- $\beta$ , lamellar  $\alpha$  and equiaxed  $\alpha$  grains. The main focus of this paper is the investigation of the effects of equiaxed  $\alpha$  grains on  $\beta$  recrystallization.

### 2. Experimental Procedure

The characterization of microstructure in the  $\alpha+\beta$  temperature regime was obtained through compression testing at deformation temperatures of 1248K, 1273K and 1298K, strain rates of  $0.01\text{s}^{-1}$ ,  $0.01\text{s}^{-1}$  and  $1\text{s}^{-1}$  to a strain of 1. The thermal cycle, shown in Figure 1, consisted of a preheat treatment at the test temperature for 15min with varying post-

deformation heat treatments up to 60min followed by a water quench. Samples were sectioned along the compression axis, polished to  $0.02\mu\text{m}$  and etched with a solution of 10%HF-30% $\text{H}_2\text{O}$ -60% $\text{H}_2\text{O}_2$ . The microstructure was examined using optical microscopy with micrographs taken at the center of each specimen. Quantitative measurements were taken by converting micrographs to binary images, which were subsequently processed with image analysis software. The as-received IMI834 alloy had a composition of Ti-5.5Al-4Sn-4Zr-1Nb-0.3Mo-0.5Si-0.06C (wt%) with a bimodal  $\alpha+\beta$  microstructure of ~20% equiaxed  $\alpha$  within a transformed  $\beta$  matrix, shown in Figure 2.

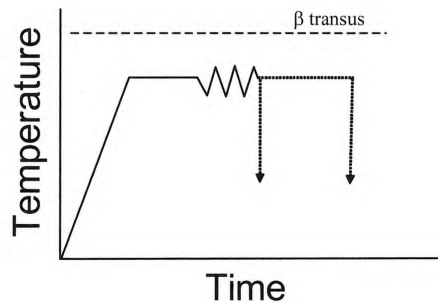


**Figure 1.** Schematic of general thermal cycle.

### 3. Results

Typical stress-strain curves, shown in Figure 3 for 1298K and 1248K, display a peak strain of ~0.05 followed by flow softening until steady state stress was reached at large strain (0.8). The level of flow softening was ~30% for 1248K at  $1\text{s}^{-1}$ .

In general, the initial microstructure at 1298K, shown in Figure 4, consists of a matrix of equiaxed  $\beta$  grains (average grain size,  $d_{\text{avg}}=50\ \mu\text{m}$ ), appearing as martensite due to the transformation upon quenching to room temperature. Equiaxed  $\alpha$  grains ( $d_{\text{avg}}=18$

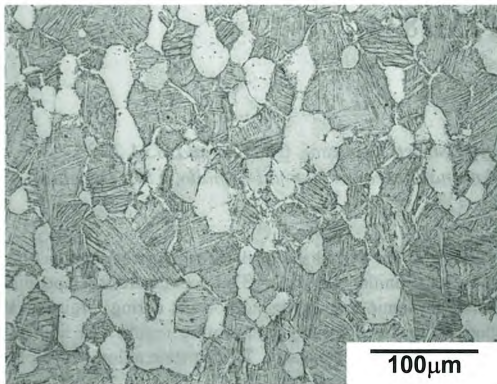


Figure 2. As-received IMI834 with a bimodal  $\alpha$ + $\beta$  microstructure.

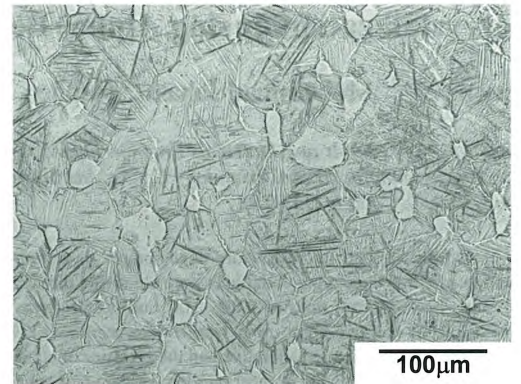


Figure 4. Microstructure after 15min preheat treatment at 1298K.

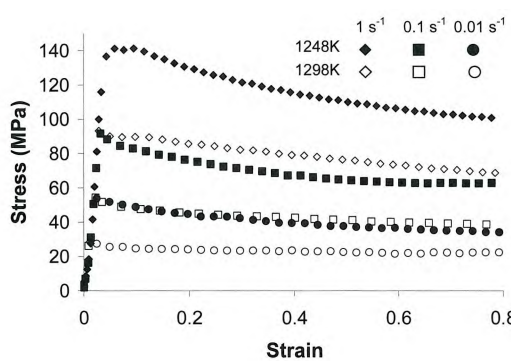


Figure 3. Stress-strain curves at 1248K and 1298K.

$\mu\text{m}$ ) are located on prior- $\beta$  grain boundaries (characterized by grain boundary  $\alpha$ ), comprising approximately 8% of the structure. The as-deformed microstructure, shown in Figure 5, displayed dynamic recrystallized prior- $\beta$  grains located at pancaked prior- $\beta$  grain boundaries and in zones adjacent to equiaxed  $\alpha$  grains. Recrystallized grains were seldom in areas devoid of equiaxed  $\alpha$  while none was observed within the prior- $\beta$  grains. At 1298K, the level of recrystallization was measured at 10% and 24% at strain rates of  $0.01\text{s}^{-1}$  and  $1\text{s}^{-1}$ . Equiaxed  $\alpha$  grains appear relatively unchanged as evidenced by a minor increase in aspect ratio from 1.7 to 2.2.

In general, deformation at 1273K produced similar microstructures to those obtained at 1298K, although the phase fractions and level of recrystallization increased to approximately 15% and 36% (at  $1\text{s}^{-1}$ ), respectively. A post deformation heat treatment was necessary to obtain completely refined microstructures at 1273K and 1298K, with annealing times dependent on temperature and strain rate. Annealing for an additional 40s after deformation at 1273K produced 60% and 100% recrystallization for strain rates of  $0.1\text{s}^{-1}$  and  $1\text{s}^{-1}$ , respectively.

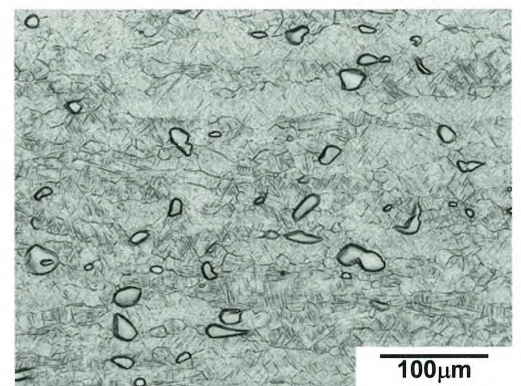
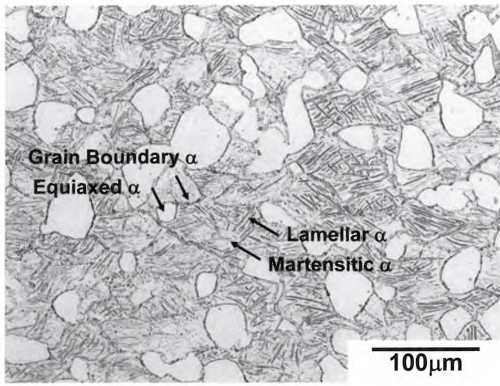


Figure 5. Microstructure after deformation at 1298K and  $1\text{s}^{-1}$ .

At 1248K, the transformed  $\beta$  matrix of the as-received material is not completely re-transformed to the  $\beta$  phase during the preheat treatment. Consequently, the pre-deformation microstructure contains lamellar  $\alpha$  within the interior of  $\beta$  grains as well as equiaxed  $\alpha$  at  $\beta$  grain boundaries. These features are also clearly distinguishable in the dead zones of the as-deformed specimen, as shown in Figure 6. After deformation, lamellar  $\alpha$  appears bent or sheared and are oriented approximately transverse to the compression axis, as shown in Figure 7 for a strain rate of  $1\text{s}^{-1}$ . In the as-deformed microstructure, grain boundary  $\alpha$  is not distinguishable from lamellar  $\alpha$ . As a result,  $\beta$  recrystallization was not analyzed at 1248K. Full globularization of the lamellar  $\alpha$  was achieved with a post-deformation heat treatment of 60min.

#### 4. Discussion

The flow behavior in the two-phase  $\alpha$ + $\beta$  temperature regime is consistent with the observed microstructure development. The increase in flow



**Figure 6.** Microstructure after deformation at 1248K and  $1\text{s}^{-1}$  at the top of specimen (dead zone).

stress with decreasing temperature is due not only to slower diffusion and more difficult slip, but also in part to the increase in  $\alpha$  phase fraction from 8% at 1298K to 25% at 1248K. Flow softening during deformation can be attributed to dynamic recrystallization at higher temperature ( $\geq 1273\text{K}$ ) and the bending/shearing of lamellar  $\alpha$  at lower temperature<sup>2,6</sup>.

Complete dynamic recrystallization was not achieved under tested temperature and strain rate conditions due to the fast recovery promoted by the high stacking fault energy and rapid self-diffusion of the body centered cubic (bcc)  $\beta$  phase<sup>3</sup>. With decreasing strain rates, recrystallization was reduced as sufficient time is available for recovery processes to reduce the accumulated dislocation density and subsequent driving force for  $\beta$  recrystallization. With decreasing temperature ( $1298\text{K} \rightarrow 1273\text{K}$ ), recrystallization is increased. However, the effect of temperature on recrystallization requires the parallel consideration of the  $\alpha/\beta$  phase transformation.

In the ideal case of a uniform alloy composition under equilibrium conditions, the  $\alpha/\beta$  phase fraction may be predicted using a  $\beta$  approach curve<sup>7</sup>, which displays the phase fraction as a function of temperature. In practice though, casting defects such as beta flecks and tree rings, produced by element segregation (between the solid/liquid phases) and non-uniform control (from variations in the electric arc, stirring, etc.), respectively, result in compositional variations that will affect the  $\beta$  transus temperature<sup>1</sup>. In addition, preheat treatment times may not be sufficient to achieve equilibrium under all conditions<sup>4</sup>, which would result in phase transformation concurrent with deformation. The effect of non-transformed  $\alpha$  in the matrix, which is present as lamellar  $\alpha$ , is considered later for low temperature deformation (1248K).

The presence of equiaxed  $\alpha$  in the pre-deformation microstructure increases the fraction of recrystallization, which can be attributed to a refined initial  $\beta$  grain size. Recrystallization is accelerated

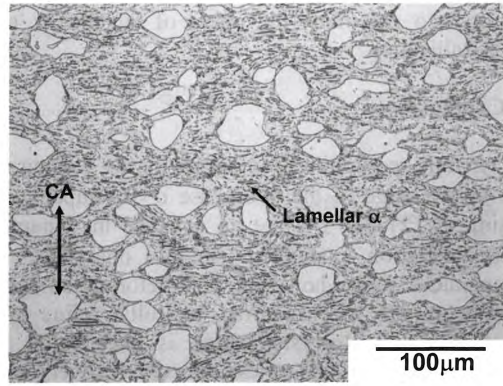


**Figure 7.** Microstructure after deformation at 1248K and  $1\text{s}^{-1}$  at the center of specimen.

in a fine-grained compared to a coarse-grained initial structure due to an increase in grain boundary area and therefore nucleation sites<sup>8</sup>. The equiaxed  $\alpha$  volume fraction and mean grain size imposes a limit to  $\beta$  grain size<sup>2</sup>.

The association of recrystallized regions with equiaxed  $\alpha$  grains indicates that  $\alpha/\beta$  boundaries serve as favorable nucleation sites. Nucleation may be stimulated due to the formation of inhomogeneities at second phase particles during deformation<sup>8</sup>. A finite element simulation of the stress state within  $\alpha+\beta$  Ti-6Al-4V revealed that  $\alpha/\beta$  phase boundaries, which feature differing mechanical properties and crystallographic orientations, display a greater stress gradient than  $\beta/\beta$  grain boundaries<sup>9</sup>. Nucleation of recrystallized grains mainly at phase boundaries has also been reported in duplex  $\alpha+\beta$  brass alloys<sup>8</sup>.

The difference in flow behavior between phases increases in significance with increasing equiaxed  $\alpha$ . Self-consistent modeling predicts the greater accommodation of strain within the  $\beta$  matrix relative to equiaxed  $\alpha$  grains, which is evidenced by the appearance of un-deformed equiaxed  $\alpha$  in the deformed microstructures<sup>4</sup>. The greater strain in the  $\beta$  matrix when equiaxed  $\alpha$  is present (compared to a fully  $\beta$  structure) increases the amount of stored energy available for recrystallization.

The inability to distinguish between grain boundary  $\alpha$  and lamellar  $\alpha$  under optical microscopy prevented the experimental characterization of recrystallization after deformation at low temperature (1248K). However the break-up, and subsequent globularization after heat treatment, of lamellar  $\alpha$  is evidence of significant strain partitioning between  $\beta$  grains and lamellar  $\alpha$  (with equiaxed  $\alpha$  behaving as hard inclusions in a soft matrix). The mechanism of globularization involves the penetration of  $\alpha/\alpha$  interfaces by the  $\beta$  phase and has been attributed to  $\alpha$  recrystallization, shearing and/or subgrain formation<sup>6</sup>. Further investigation is

required to determine the effect of lamellar  $\alpha$  on recrystallization.

## 5. Conclusions

Dynamic recrystallization occurs during forging in the upper range of the two-phase  $\alpha+\beta$  temperature regime ( $\geq 1273\text{K}$ ). Despite an increase in dynamic recrystallization compared to the one-phase  $\beta$  temperature range however, post-deformation heat treatments are still required to fully refine the microstructure. Recrystallization is accelerated at lower temperature due to less effective recovery and the presence of equiaxed  $\alpha$ , which limits the initial prior- $\beta$  grain size. As a result, temperature control during forging is critical, particularly near the  $\beta$  transus, in order to obtain a minimum fraction of equiaxed  $\alpha$  in the initial microstructure.

## Acknowledgement

The authors wish to acknowledge the funding provided by National Sciences and Engineering Research Council of Canada (NSERC) and the contributions of the Aerospace Manufacturing Technology Center, Institute of Aerospace Research, National Research Council Canada (AMTC-IAR-NRC).

## REFERENCES

- 1) S.L. Semiatin, V. Seetharaman and I. Weiss: *Advances in the Science and Technology of Titanium Alloy Processing*, ed. by I. Weiss, R. Srinivasan, P.J. Bania, D. Eylon and S.L. Semiatin, (TMS, Warrendale PA, 1997) pp.3-73.
- 2) R.W. Evans, G.S. Clark and S.G. McKenzie: *MECAMAT'91 Large Plastic Deformations: Fundamental Aspects and Applications to Metal Forming*, ed. by C. Teodosiu, J.L. Raphanel
- 3) H.M. Flower: Mater. Sci. Technol. **6** (1990) pp. 1082-1092.
- and F. Sidoroff, (A.A. Balkema, Rotterdam, 1993) pp. 395-403.
- 4) P. Vo, M. Jahazi, S. Yue and P. Bocher: Mater. Sci. Eng. A **447** (2007) pp. 99-110.
- 5) P. Vo, M. Jahazi and S. Yue: Advanced Materials Research **15-17** (2007) pp. 965-970.
- 6) E.B. Shell and S.L. Semiatin: Metall. Mater. Trans. **30A** (1999) pp. 3219-3229.
- 7) D.F. Neal: *Materials Design Approaches and Experiences*, ed. by J.-C. Zhao, M. Fahrmann and T.M. Pollock, (TMS, Warrendale, 2001) pp. 199-213.
- 8) F.J. Humphreys and M. Hatherly: *Recrystallization and Related Annealing Phenomena*, (Elsevier Science Ltd, Oxford, 1996) pp. 173-220,277-279
- 9) Z.X. Guo and R. Ding: *Ti-2003 Science and Technology*, ed. by G. Lutjering and J. Albrecht, (Wiley-VCH, Weinheim, 2004) pp. 1267-1274.